Development and validation of an optimal GATE model for proton pencil-beam scanning delivery

Asadi, Ali; Akhavanallaf, Azadeh; Hosseini, Seyed Abolfazl; Vosoughi, Naser; Zaidi, Habib

Published in:
Zeitschrift fur medizinische Physik

DOI:
10.1016/j.zemedi.2022.10.008

Document Version
Final author's version (accepted by publisher, after peer review)

Publication date:
2022

SHORT COMMUNICATION

Development and validation of an optimal GATE model for proton pencil-beam scanning delivery

Ali Asadi [a], **Azadeh Akhavanallaf** [b], **Seyed Abolfazl Hosseini** [a,*], **Naser Vosoughi** [a], **Habib Zaidi** [b,c,d,e,*]

[a] Department of Energy Engineering, Sharif University of Technology, Tehran, Iran
[b] Division of Nuclear Medicine and Molecular Imaging, Geneva University Hospital, Geneva, Switzerland
[c] Geneva University Neurocenter, Geneva University, Geneva, Switzerland
[d] Department of Nuclear Medicine and Molecular Imaging, University of Groningen, University Medical Center Groningen, Groningen, the Netherlands
[e] Department of Nuclear Medicine, University of Southern Denmark, Odense, Denmark

Received 10 December 2021; accepted 14 October 2022

Abstract

Objective: To develop and validate a versatile Monte Carlo (MC)-based dose calculation engine to support MC-based dose verification of treatment planning systems (TPSs) and quality assurance (QA) workflows in proton therapy.
Methods: The GATE MC toolkit was used to simulate a fixed horizontal active scan-based proton beam delivery (SIEMENS IONTRIS). Within the nozzle, two primary and secondary dose monitors have been designed to enable the comparison of the accuracy of dose estimation from MC simulations with respect to physical QA measurements. The developed beam model was validated against a series of commissioning measurements using pinpoint chambers and 2D array ionization chambers (IC) in terms of lateral profiles and depth dose distributions. Furthermore, beam delivery module and treatment planning has been validated against the literature deploying various clinical test cases of the AAPM TG-119 (c-shape phantom) and a prostate patient.
Results: MC simulations showed excellent agreement with measurements in the lateral depth-dose parameters and spread-out Bragg peak (SOBP) characteristics within a maximum relative error of 0.95 mm in range, 1.83% in entrance to peak ratio, 0.27% in mean point-to-point dose difference, and 0.32% in peak location. The mean relative absolute difference between MC simulations and measurements in terms of absorbed dose in the SOBP region was 0.93% ± 0.88%. Clinical phantom studies showed a good agreement compared to research TPS (relative error for TG-119 planning target volume PTV-D_{95} ∼ 1.8%; and for prostate PTV-D_{95} ∼ −0.6%).
Conclusion: We successfully developed a MC model for the pencil beam scanning system, which appears reliable for dose verification of the TPS in combination with QA information, prior to patient treatment.

Keywords: Proton therapy; Monte Carlo simulation; active scanning; AAPM TG-119; prostate

1 Introduction

There is a globally growing interest in using different types of particles (such as protons and Carbon ions) compared to conventional radiation therapy owing to the inherent potentials of particles in dose-painting through escalating the delivered dose to target while sparing normal tissues [1–3]. Nowadays, active scanning proton therapy

* Corresponding authors: Habib Zaidi, Ph.D., Geneva University Hospital, Division of Nuclear Medicine and Molecular Imaging, CH-1211 Geneva, Switzerland and Seyed A. Hosseini, Ph.D, Sharif University of Technology, Department of Energy Engineering, Tehran, Iran.
E-mail addresses: sahosseini@sharif.edu (S. A. Hosseini), habib.zaidi@hcuge.ch (H. Zaidi).

Z Med Phys **xxx** (2022) xxx–xxx
https://doi.org/10.1016/j.zemedi.2022.10.008
www.elsevier.com/locate/zemedi

(PT), referred to as pencil beam system (PBS), has become a reliable and preferred method for cancer treatment compared to conventional passive scattering PT (PSPT) technique, owing to major advantages in terms of conformal dose distributions and hence facilitating beam delivery without the need for multiple field-specific scatterer mechanical hardware [4,5]. Commercially available PT facilities employ mainly semi-analytic algorithms for dose planning. TPS simplifications incorporated in dose planning in complex situations, including utilization of aperture (reducing the lateral penumbra) or range shifter (RS) (shallow tumor treatments), may lead to large errors between the prescribed dose and delivered dose. For instance, Nichiporov et al. [6] studied the range shift and dose perturbation caused by Al, Ti and Cu exposed to proton beams at various energies. In particular, for 10 mm Ti, the difference between the calculated and measured range was 0.1 mm for an exposure at high energy (194 MeV), whereas the dose perturbation factor was 1.025 in the spread–out Bragg peak region (SOBP). For other materials, the difference of 0.3 mm between calculated and measured range was obtained. To ensure correct delivery of the planned dose through TPS, pre-treatment dose verifications, called patient-specific QA, are recommended for clinical workflows [7,8]. However, due to the growing demand for PT and the increased treatment time, such procedures are less feasible in routine clinical practice. In this context, independently benchmarked and validated MC simulation tools can be properly utilized for patient-specific dose monitoring prior to treatment. In this regard, various MC codes, including FLUKA [9–11], MCNP [12,13], Geant4 [14,15], and some MC toolkits, such as GATE and TOPAS [16,17] have been utilized for proton beam delivery simulation, allowing users to validate and examine various aspects of beam-material interactions [18–24]. A substantial body of literature reported on the various MC models developed for both passive scattering and active scanning systems of cyclotron and synchrotron-based PT facilities. In particular, Fiorini et al. [25] used Fluka MC code for the simulation of cyclotron-based clinical scanning machine. They reported that compared to experimental measurements, their MC simulations produces more stable results with smaller bias and lower variance than those obtained from the TPS. Hence, they proposed to use MC-based calculations for the evaluation of dosimetric parameters in PT facilities. Fracchiolla et al. [26] used TOPAS MC toolkit to validate a MC model of a machine using only commissioning measurements by avoiding nozzle modeling. Their proposed MC model achieved reasonable results in the validation phase, for both simple irradiation geometries (SOBP in water) and modulated treatment fields. In addition, both MC and TPS results were compared with experimental measurements with and without RS in terms of Gamma index. MC modeling reached >95% and >93% Gamma pass rate with and without RS, respectively. Prusator et al. [27] developed a simulation model of a compact PT unit with TOPAS MC toolkit. They reported dosimetric parameters, such as Integrated Radial profiles as function of Depth (IRDP), SOBP, and lateral profile of dose distributions compared with experimental measurements. The results show that TOPAS MC toolkit can reproduce the introduced parameters with a difference of 0.1 cm in range, and SOBP width with 0.3 cm accuracy, and came up concluding that the use of MC simulations can be a viable tool in the verification of proton treatment planning. Hamad et al. [28] studied the simulation of Bragg-curves of Carbon ions using the Geant4 MC toolkit whereas Padilla-Cabal et al. [29] used GATE/Geant4 MC code for the simulation of proton pencil beam within a magnetic field. In this study, MC simulations reached 0.2 mm difference in range and 1.2% deviation of dose with respect to experimental measurements. The results of this study showed that GATE can be used as a QA tool in the Magnetic resonance guidance in PT (MRPT) process Almhagen et al. [30] simulated an active proton scanning design to investigate the potential of MC-based models in software QA and patient-motion studies. Grevillot et al. [31] developed a MC-based simulator for modeling the Ion Beam Application (IBA) active scanning PT system using Beam Data Library [31]. They reported a slight difference between the simulation results with respect to experimental measurements using 2D-array IC. Fuchs et al. [32] developed a computer-driven approach allowing for a simple generation of a MC beam model of a scanned beam delivery system using the GATE-RTion MC toolkit. Their results showed a reasonable agreement between simulations and measurements, and the developed method can be used by non-expert users in the field.

In this work, we developed a unified framework for patient-specific QA framework based on the GATE MC toolkit. A dosimetric comparison between simulation results and experimental measurements using pinpoint chambers and 2D-array IC was performed for validation and benchmarking. Furthermore, we validated our MC simulator using two homogeneous phantoms and examined the simulation results in terms of dose volume histogram (DVH) parameters against the results available from matRad TPS [33] for the prostate and TG-119 phantom. matRad is an open-source research TPS written in Matlab based on modified pencil-beam algorithms [34–36] and a set of MC calculated physical database for dose calculation [34].

2 Materials and methods

2.1 System description

The Shanghai Advanced PT (SAPT) facility, a synchrotron-based active scanning PT system, was

Please cite this article as: A. Asadi, A. Akhavanallaf, S.A. Hosseini et al., Development and validation of an optimal GATE model for proton pencil-beam scanning delivery, Z Med Phys, https://doi.org/10.1016/j.zemedi.2022.10.008

simulated in this work. Fig 1 depicts the geometrical characteristics of the SIEMENS IONTRIS system installed at SAPT. In this system, proton beams are extracted from a synchrotron and drifted to the nozzle using paired scanning magnets in the horizontal (X) and vertical (Y) directions that can scan/guide the beam laterally on the target. The proton beam spot is moved in the isocenter using the energy stacking technique to cover the target volume at depth. The energy of this system varies between 70 and 235 MeV [37,38]. In addition, in case of surface treatment, a 2 cm PMMA shifter is incorporated in this system [38]. The characteristics of this system are summarized in Table 1.

The proton beam is monitored in real time using two parallel-plate IC. The spot size and beam optics are measured using position detectors. Unlike discrete scan mode (pixel scan), IONTRIS provides a continuous beam scan mode (raster scan).

Table 1
The main characteristics of the SAPT system [37].

Item	Value
Energy (MeV)	70–235
Field size (cm^2)	40 × 30
Scanning magnet x to isocenter distance (cm)	287
Scanning magnet y to isocenter distance (cm)	242
Nozzle to isocenter distance (cm)	40
Average scan speed in x (cm/ms)	2
Average scan speed in y (cm/ms)	0.5
Dose rate (Gy/min)	2

2.2 GATE simulations

In this study, The GATE v8.2 MC code alongside with GEANT4 10.5 p01 was employed since it has been previously validated for clinical operation of particle therapy systems [31]. The proton beam and monitoring devices have been simulated based on the method proposed by Grevilot et al. [31]. The initial beam (source plane) was set at the nozzle entrance immediately in front of the vacuum window. The angular spread particle sampling strategy was adopted. The geometry of the ion chamber was simplified to consist of water with the corresponding water equivalent depth reported by the manufacturer. Following the approach described by Parodi et al. [22], the multi-wire proportional chamber (MWPC) was described as water covered by a 3-micrometer Tungsten layer representing scattering of low energy protons in the high-Z Tungsten wires. The simulation process was performed with a set of pre-built Geant4 physics lists examining multiple values for production cuts on secondary products, and step sizes of protons in the water phantom. The dose-depth metrics obtained from simulations were compared to measurements taken from clinical commissioning of SAPT facility to fine-tune the input simulation parameters.

According to previous studies, QGSP_BIC module has been deployed to model hadronic interactions whereas EMZ (EM stand for Electromagnetic) was used to consider electromagnetic processes based on the G4EMStandardPhysics_Option4 module [31,39]. In addition, different values for ionization potential of water have been reported to directly influence the simulation results [40–45]. The value of the mean excitation energy for water recommended in the ICRU report 90 (I=78 ev) was adopted [46–48].

Another parameter that has a direct effect on the accuracy of calculations and computational time is the cut-off value for production cuts on secondary particles (electrons, photons, positrons) after EM interactions. In the water phantom, we selected different cut-off values varying between 0.001 mm and 0.225 mm. The results showed that selecting a cut-off value of less than 0.1 mm always leads to an error of less than 2.1% in the estimates. Similar to the work of Grevillot et al. [31,43,49,50] and Elia et al.[41,42], we considered a cut-off value of 0.1 mm for particle transport of secondary particles (electrons, photons, positrons) after EM interactions in the water phantom. The cut-off value for

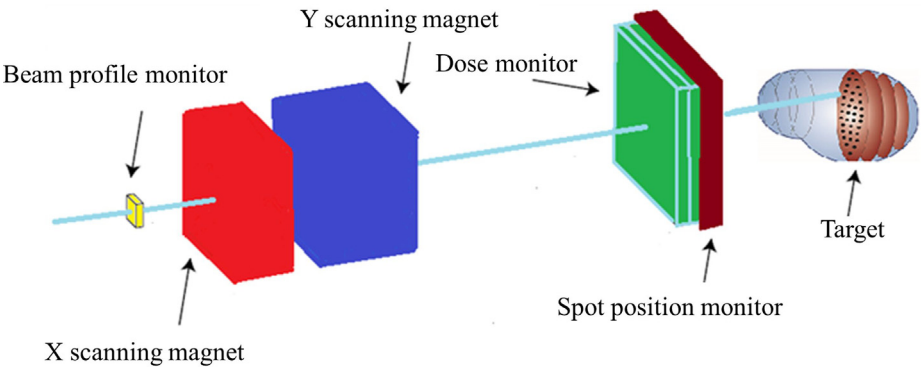

Figure 1. Simple schematic illustration of the SAPT nozzle [37].

particle transport was set to 0.075 mm and 0.025 mm for secondary particles (electrons, photons, positrons) in the TG-119 and the prostate phantom, respectively. In addition, the maximum step limiter of protons was set to 0.1 mm in the water, TG-119, and prostate phantoms. Fig. 2 illustrates schematically the simulation workflow. In this study, case-specific dose modeling was conducted in three main parts: (a) feeding phantom (water or patient anatomical image) geometry into the simulator using the calibration curve of Hounsfield Unit (HU)-to-mass density and accordingly the density map is internally converted into RSP using G4EMcalculator module [50,51]; (b) treatment plan optimization using the irradiation criteria (prescribed dose to target and restrictions) and contours obtained from DICOMRT-structure; and (c) recording 3D dose map and extracting clinically relevant dose-volume parameters.

2.3 Beam characterization and simulation validation

The developed MC simulator was benchmarked against the experimental measurements reported by Shu et al. [37] and Sheng et al. [38] and a clinical case study extracted from the Sánchez-Parcerisa study [33].

2.3.1 Integral radiation profiles as a function of depth (IRPDs)

The dose distribution curves for seven energies in the range from 70 to 235 MeV were obtained using the water phantom (MP3-PL, PTW, Freiburg, Germany) with a large diameter parallel plate chamber (Bragg peak chamber Model 34070, PTW) with a nominal sensitive chamber volume of 10.5 cm in diameter and water equivalent thickness ≈ 4 mm. The PEAKFINDER device with a radius of 4.08 cm was positioned at 5 cm downstream from the nozzle exit. The energy of the simulated proton beams was adjusted between 70 and 235 MeV. In the measurement, the range (defined as R80) for each IRPD and the clinical range parameter (R90) were calculated [31].

2.3.2 Optical properties

In the measurements reported by [37,38], a Gafchromic film was used to quantify the beam spot on the lateral profile (full-width at half-maximum (FWHM) in X and Y directions) to benchmark the simulation in terms of spot size, where a total of 7 energy spot sizes were calculated. The proton beam was defined as a point source, while a Gaussian-shaped beam angular spread in X and Y directions was implemented in the simulation. 2D dose distributions were scored at the same locations. The resolution of scoring along the central beam axis was set to 0.36 mm to match the spacing of measurements. The angular spread in the X and Y directions was adjusted to match the measured FWHM. Two fourth-order polynomials were used to fit the angular spread FHWM in X and Y directions as a function of the nominal energy. The Gafchromic film was simulated through a very thin titanium plate located perpendicular to the beam path and the spot size were extracted from the particle phase space using the Gate Phasespace Actor attached to planes corresponding to the measured location around isocenter (i.e. the isocenter plane, 40 cm downstream isocenter, and 20 cm upstream the isocenter plane).

2.3.3 1-D dose profiles in water

Range modulated plans were generated by the TPS (V13B, Syngo, Siemens) in a water tank. The targets were considered as cube, and the size of them was set to $3 \times 3 \times 3$ cm^3 and $6 \times 6 \times 6$ cm^3, and the center of this

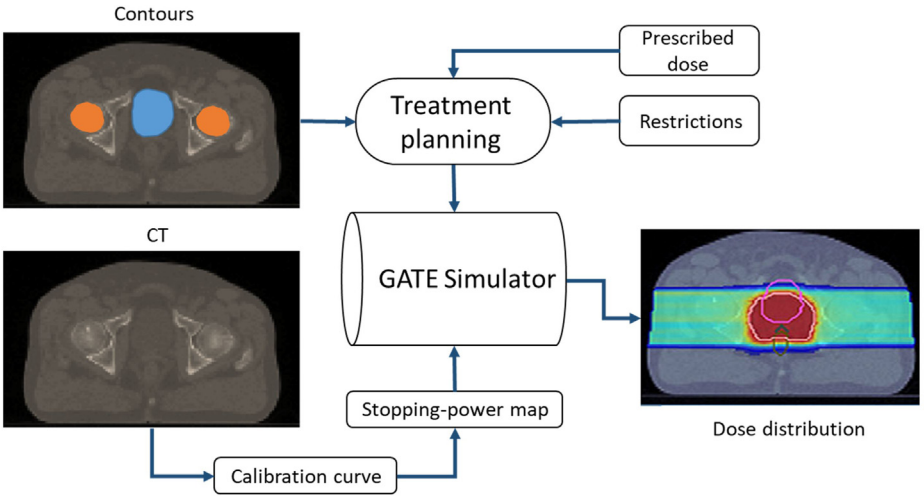

Figure 2. Schematic representation of the simulation workflow.

cubes positioned at 5 cm, and 20 cm, respectively at the main water phantom. The prescribed dose was set to 0.5 Gy. The RS was located 20 cm before the surface of the water tank for the range modulated plan with a shallow target. The plan was delivered to the water tank (MP3-PL, PTW, Freiburg, Germany). Measurements were performed using 24 PinPoint chambers (T31015, PTW-Freiburg) at different positions to obtain good extrapolation for depth and lateral dose profiles. Beam delivery parameters, including beam energy, scanning cosine angle for X and Y directions, particle number of each scanning spot, and the energy selection plan for modulation region were imported to the MC simulation code. The inverse planning optimization algorithm proposed by Bourhaleb et al. [52] was implemented to achieve a uniform dose to the target volume. The absorbed dose distribution per particle was scored. For measuring the lateral profile, a grid dimension was set on the 2 mm^2, whereas it was set to 0.1 mm for the Z axis (in depth) to measure the IRDP curve. To normalize the simulation results, the routine procedure implemented within GATE software was used.

2.4 Clinical phantom study

We further validated our MC-based simulator against the matRad research TPS. This is a multimodality open-source toolkit for dose calculation and optimization in radiation therapy, that has been validated against Syngo TPS for PBS PT [33,34]. Clinical phantom and case studies reported by Sánchez-Parcerisa et al. [33] were modeled and compared against the published reference. AAPM (TG-119) C-shape phantom imported to the GATE TPS source, where the C-shape PTV intricate around a core structure whose outer surface is 0.5 cm from the inner surface of the PTV. In addition, a prostate case study, taken from Sánchez-Parcerisa et al. [33] was simulated. The structure set contains the target PTV, bladder, rectum, femur, and body. Accordingly, the TG-119 phantom was prescribed with 50 GyRBE dose to the PTV (target) and the maximum dose to the 5% of organs at risk (OARs) with 10 GyRBE (defined as GOAL) [33]. A single proton field was set on the target. A constant factor of 1.1 was applied to the physical dose to hypothesize the relative biological effect of protons. For optimization of spot and beam selection, the inverse planning optimization algorithm [52] was used to uniformly cover the target. The prostate phantom was prescribed with 78 GyRBE dose to the PTV region using 2 parallel opposed proton fields. Table 2 summarizes the radiation treatment objectives and restrictions.

Table 2
Treatment plan objectives for TG-119 [53] and prostate [54] cases.

Structure		Parameter	Goal (%)
C-shape	PTV	V10	<55
		V99	50
	Core	V5	10
Prostate	Bladder	V70	<35
		V50	<60
	Rectum	V70	<30
		V50	<50
	Femur	V50	<5

Therefore, our simulation has been benchmarked against values reported by Sánchez-Parcerisa et al. [32] in terms of DVH parameters. In the case of TG-119 test phantom, D_5 and D_{95} parameters were extracted from the DVH curve for each OAR. In the prostate clinical test case, D_2 and D_{95} for the target, D_2, and V_{70} for both bladder and rectum, and V_{50} for the femur have been compared against the reported values.

The quantitative comparison of dose-volume histogram parameters was performed based on the relative differences:

$$\mathrm{RPE} = \left(\frac{x_i - x'_i}{x_i}\right) \times 100 \quad (1)$$

where x_i and x'_i represent the DVH parameters from PBS system and Sánchez-Parcerisa et al. [33], respectively.

3 Results

3.1 Integral radiation profiles as a function of depth (IRPDs)

The difference in beam range (R80) between the simulated and experimental results for all 7 simulated energies was less than 0.95 mm. The obtained curves for 7 energies within the range 70–235 MeV (70, 130.1, 161.1, 179.9, 202, 219.2, and 235 MeV) are shown in Fig. 3. The peak to entrance dose ratio, mean point-to-point[1], Bragg-peak location, and range deviation between the measurements and simulation results were compared (Fig. 4). The maximum deviation of the beam range between the measured and simulated results was 0.95 mm (at an energy of 235.0 MeV). The mean range deviation was also 0.33 mm. For mean point-to-point dose difference between the measurements and fitted simulation, the mean value and the maximum value were 0.21% and 0.27%, respectively. For all cases, the mean point-to-point deviation value was lower than 0.5%. The maximum peak-to-entrance dose deviation

[1] $\omega = \sum_{i=1}^{N} \left(\frac{|d_i - d_{refi}|}{d_{refi}} \times \frac{\Delta}{L} \right)$ where d_i and d_{refi} refer to simulations and measurements, respectively, Δ is the step between two points, L is the maximum range, and N is the number of data points.

Please cite this article as: A. Asadi, A. Akhavanallaf, S.A. Hosseini et al., Development and validation of an optimal GATE model for proton pencil-beam scanning delivery, Z Med Phys, https://doi.org/10.1016/j.zemedi.2022.10.008

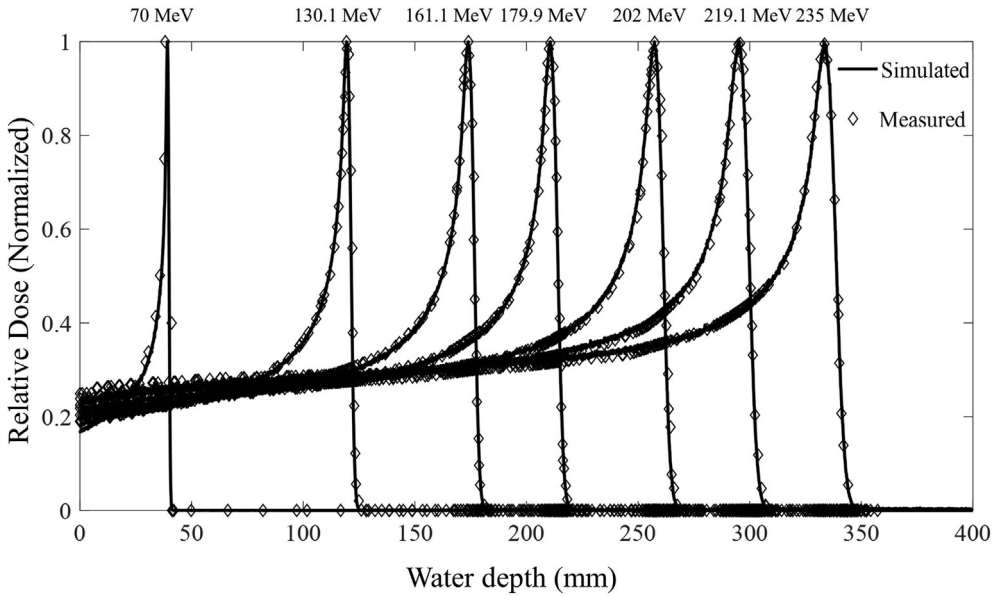

Figure 3. Comparison of simulated and measured IRPD's at different energies [37,55].

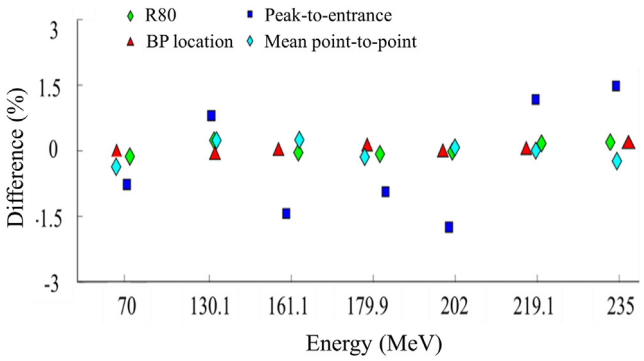

Figure 4. Comparison of range, entrance-to-peak dose ratio, mean point-to-point, and Bragg-peak location deviation between measurements and simulations [37,55].

between measurements and fitted simulation was 1.83% for proton beam energy of 202 MeV.

3.2 In air spot size

We recalculated the results based on a fitted angular distribution. The deviation between measurements and fitted simulations at the isocenter is shown in Fig. 5 (A&B). The simulated and measured spot sizes in X direction at various distances from the isocenter for two energies (121.08 MeV and 221.07 MeV) were presented in Fig. 5C. The mean difference of FWHM was 2.82% at the isocenter, whereas its maximum difference was 6.5% at 160.1 MeV proton energy in the X direction. The mean relative difference of FWHM was 5.22% at the isocenter, whereas the maximum difference was 16.4% at proton energy of 160.1 MeV in the Y direction. The spot size was reproduced within ±0.7 mm for two positions around the isocenter, where the differences were about −4.52% and 4.2% at 40 cm downstream of the isocenter and 0.18% and 0.34% at 20 cm upstream of the isocenter for energies of 221.07 MeV, and 121.8 MeV, respectively.

3.3 Comparison of 1-D dose profiles

Measured and MC-simulated depth-dose curves along the central axis and transverse beam profile at the center of the SOBP cubes are shown in Fig. 6. The results show good agreement between simulations and measurements. The clinical range difference was 0.22 mm and the 80–20% distal fall off value difference was 0.11 mm. The mean (SD) and maximum dose differences of the depth dose profile were 0.93% (0.88%) and 3.53%, respectively, for the measured points except for points at the distal edge of the SOBP. The dose differences of the lateral dose profile between simulations and measurements at the FWHM dose level were within 2.30%.

3.4 Clinical phantom evaluation

Fig. 7 shows the dose distribution for TG-119 phantom and a prostate case for the PBS PT plan along with DVH analysis for the target region and OARs. The color wash is normalized (TG-119: 30 fractions, each 1.66 Gy, and pros-

Please cite this article as: A. Asadi, A. Akhavanallaf, S.A. Hosseini et al., Development and validation of an optimal GATE model for proton pencil-beam scanning delivery, Z Med Phys, https://doi.org/10.1016/j.zemedi.2022.10.008

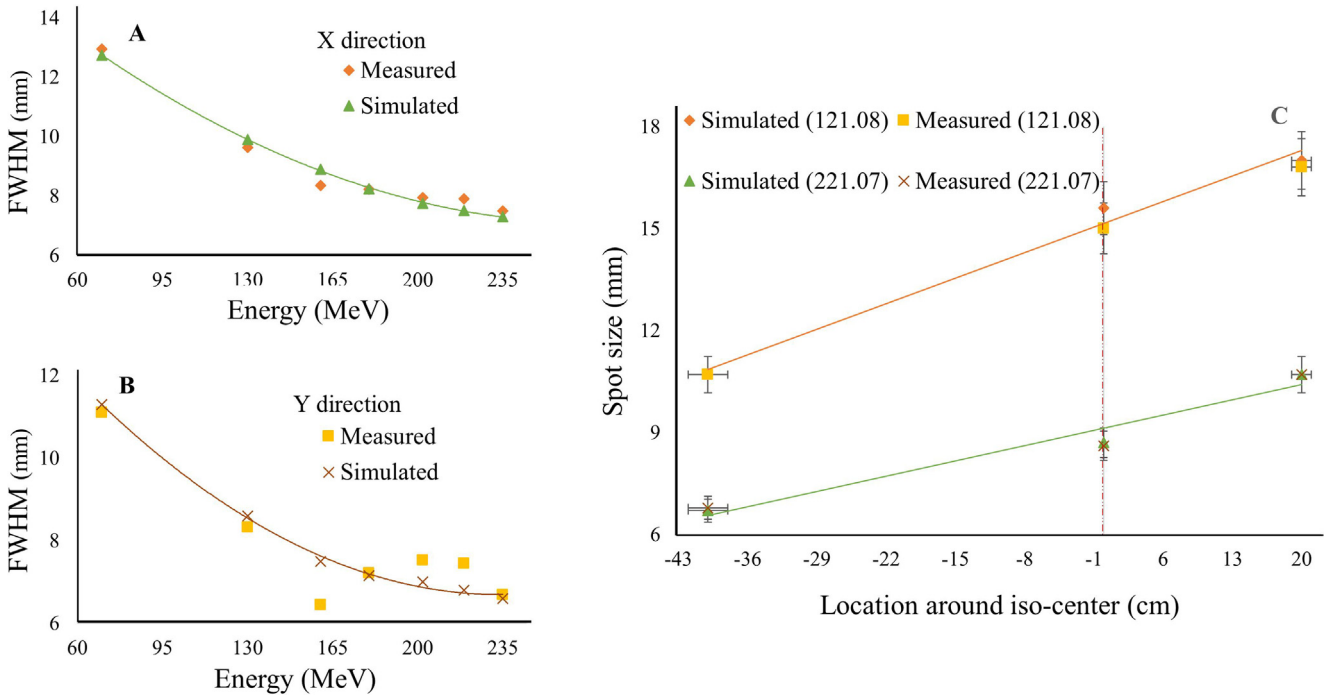

Figure 5. Differences between simulated and measured spot size at the isocenter for both (A) X and (B) Y directions for different energies. (C) Sample of the simulated and measured spot sizes in X direction for energies of 121.08 and 221.07 MeV at different locations around the isocenter [55].

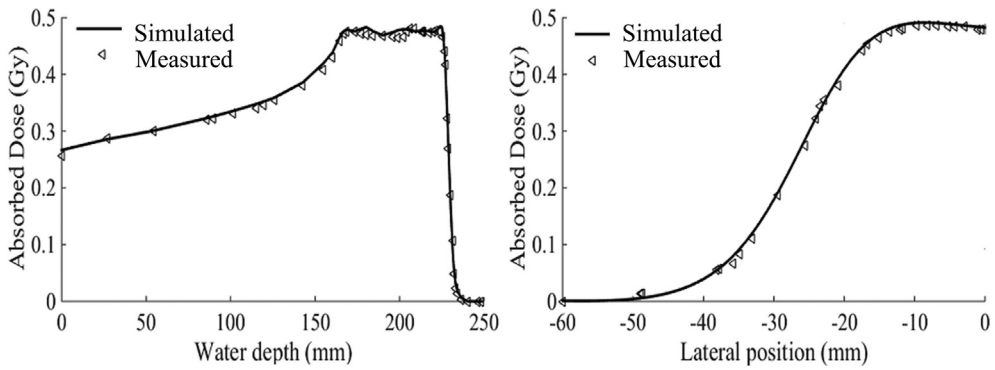

Figure 6. Comparison of the SOBP plan for (a) a longitudinal profile and (b) a transverse profile at the center of the water-filled phantom [55].

tate case: 78 Gy in 39 fractions). Tables 3 and 4 represent the DVH-driven parameters obtained from simulations compared to results reported in [33].

4 Discussion

The SAPT system was modeled and simulated using the GATE MC toolkit. The accuracy of the simulations was validated through comparisons against experimental measurements for multiple parameters based on measurements of the transverse profile of the absorbed dose in the water phantom, and optical properties in air.

The results showed that there is a good agreement between simulations and experimental measurements. The mean deviation of the simulated absorbed dose at the SOBP region from the corresponding measurements was about 0.93%, which is in agreement with previous studies where the same order of error magnitude (between 1% and 3%)

Please cite this article as: A. Asadi, A. Akhavanallaf, S.A. Hosseini et al., Development and validation of an optimal GATE model for proton pencil-beam scanning delivery, Z Med Phys, https://doi.org/10.1016/j.zemedi.2022.10.008

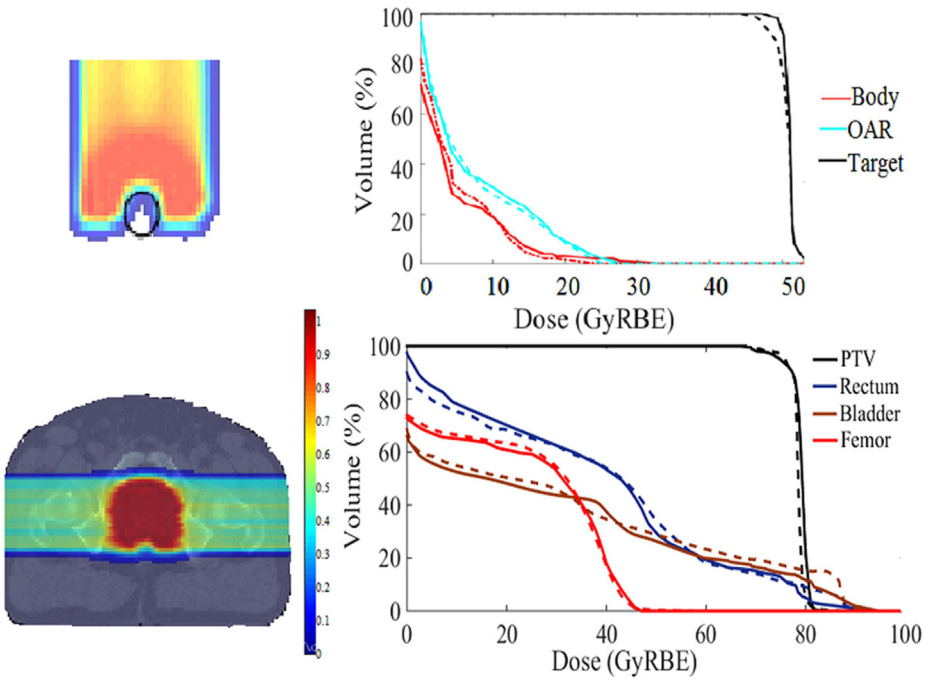

Figure 7. Simulated **d**ose distribution for TG-119 phantom (top) and prostate (bottom) cases in the PBS PT plan along with DVH plots for target and OARs (solid line, simulation) compared to Ref. [33] (dash line).

Table 3
Quantitative analysis for DVH parameters in the TG-119 phantom.

ROI	D_5 (Gy)			D_{95} (Gy)		
	Simulation	Sánchez-Parcerisa et al. [33]	Diff. (%)	Simulation	Sánchez-Parcerisa et al. [33]	Diff (%)
Target	52.25	49.4	5.4	50.3	49.4	1.8
OAR	12.3	11.3	8	0	0	0

Table 4
Quantitative analysis for DVH parameters in the prostate case clinical study.

Structure		Sánchez-Parcerisa et al. [33]	Simulation	Diff. (%)
Target	D_2 (Gy)	81.0	81.4	−0.40
	D_{95} (Gy)	75.5	75.0	0.66
Bladder	D_2 (Gy)	87.1	87.2	0.1
	V_{70} (Gy)	19.36	19.5	0.72
Rectum	D_2 (Gy)	88	82.1	6.7
	V_{70} (%)	11.6	11.9	−2.58
Femur	V_{50} (%)	0	0	0

was reported [42,56]. The deviation between the measured and simulated range was less than 0.95 mm. Elia et al. [42] reported 0.2 and 0.3 mm range deviation with and without RS between simulations and experiments. In addition, Almhagen et al. [30] reported a maximum error of 0.2 mm in range simulation, and Fracchiolla et al. [26] used the TOPAS MC code for modeling the PBS system and reported a range difference lower than 1.1 mm. We calculated a slightly higher deviation between simulated and measured peak to entrance dose (−1.83%) compared to Elia et al. (0.4%) [42]. Moreover, Fig. 4 shows that the deviation in the range, BP location, and peak-to-entrance dose ratio between the measured and simulated results increased with increasing the energy. In fact, the selected physics list has

Please cite this article as: A. Asadi, A. Akhavanallaf, S.A. Hosseini et al., Development and validation of an optimal GATE model for proton pencil-beam scanning delivery, Z Med Phys, https://doi.org/10.1016/j.zemedi.2022.10.008

a nuclear part and an electromagnetic part, and it can be said that with increasing the energy, the cross-section of the nuclear part increases, and this factor will cause a deviation by under/over-estimating the simulations results. The maximum deviation between the simulated and experimentally measured spot size was about −4.52% (40 cm downstream of the isocenter at 221.07 MeV). Fracchiolla et al. [26] reached an average error of 4% in FWHM estimation, whereas Elia et al. [41] reported a larger deviation corresponding to 7.2%, and 6.9% in the vertical and horizontal planes, respectively. The observed deviation in FWHM particularly for energies higher than 160 MeV can be justified by the production of secondary particles, especially electrons. The explanation regarding the impact of increasing the nuclear reactions cross-section at higher energies will also be true here. In fact, the increase in the cross-sectional area causes the production of secondary particles to be estimated, but the production of these particles is not symmetrical. This asymmetry makes it difficult to measure the spot size and FWHM for an observer who considers the same criterion for all energies. Hence, a relatively higher deviation occurs in the FWHM measurement. According to Grevillot et al. [31], deviations within 5% between simulated and measured parameters are within acceptable limits for QA applications.

We further validated our MC simulations against a research TPS using phantom and clinical studies. The results showed that the simulated results obtained from GATE combined with the treatment planning algorithm agree well with experimental measurements and theoretical evaluations. In the TG-119 phantom study, we observed a slightly higher deviation between our results and those reported by Sánchez-Parcerisa et al. [33] (∼6.7%). This deviation particularly in clinical target volume boundaries dose (dose to core) stems mainly from the dosimetry method. matRad has several dose calculation algorithms that consider variable relative biological effect (RBE) for protons, contrary to the above reference which used the multiRBE model in their simulations, we applied a constant factor of 1.1 as RBE of protons, which influences mainly the out-of-field dose.

5 Conclusion

The presented MC-based simulator has been developed for dose calculation in PBS PT. The simulated plans for water phantoms and in air studies agree well with experimental measurements performed using various detectors used in system calibration and validation studies [37,38]. We further validated our MC simulations against a research TPS using two homogenous phantoms. The results showed that the simulated results obtained from GATE combined with the treatment planning algorithm agree well with the TPS results in the term of DVH and related parameters. The obtained results prove the capability of the developed simulator as an independent software QA program that can be implemented and adopted in the clinical workflow.

Declaration of Competing Interest

The authors declare that they have no known competing financial interests or personal relationships that could have appeared to influence the work reported in this paper.

Acknowledgements

This work was supported by Sharif University of Technology and the Swiss National Science Foundation under grant SNRF 320030_176052.

References

[1] Lomax A. Intensity modulation methods for proton radiotherapy. Phys Med Biol 1999;44(1):185.
[2] Paganetti H et al.. Roadmap: proton therapy physics and biology. Phys Med Biol 2021;66(5):p. 05RM01.
[3] Parodi K. Latest developments in in-vivo imaging for proton therapy. Br J Radiol 2020;93(1107):20190787.
[4] Loeffler JS, Durante M. Charged particle therapy—optimization, challenges and future directions. Nat Rev Clin Oncol 2013;10 (7):411–424.
[5] Pedroni E et al.. Initial experience of using an active beam delivery technique at PSI. Strahlenther Onkol 1999;175(2):18–20.
[6] Nichiporov D et al.. Range shift and dose perturbation with high-density materials in proton beam therapy. Nucl Instrum Methods Phys Res, Sect B 2011;269(22):2685–2692.
[7] Arjomandy B et al.. Verification of patient-specific dose distributions in proton therapy using a commercial two-dimensional ion chamber array. Med Phys 2010;37(11):5831–5837.
[8] Zhu XR et al.. Patient-specific quality assurance for prostate cancer patients receiving spot scanning proton therapy using single-field uniform dose. Int J Radiat Oncol Biol Phys 2011;81(2):552–559.
[9] Battistoni G et al.. The FLUKA code: an accurate simulation tool for particle therapy. Front Oncol 2016;6:116.
[10] Ferrari A, et al. FLUKA: A multi-particle transport code (Program version 2005): Cern; 2005.
[11] Aiginger H et al.. The FLUKA code: New developments and application to 1 GeV/n iron beams. Adv Space Res 2005;35 (2):214–222.
[12] Ryckman JM. Using MCNPX to calculate primary and secondary dose in proton therapy. Georgia Institute of Technology; 2011.
[13] Waters LS et al.. The MCNPX Monte Carlo radiation transport code. Hadronic Shower Simulation Workshop 2007;896:81–90.
[14] Allison J et al.. Geant4 developments and applications. IEEE Trans Nucl Sci 2006;53(1):270–278.
[15] Allison J et al.. Recent developments in Geant4. Nucl Instr Meth A 2016;835:186–225.
[16] Perl J et al.. TOPAS: an innovative proton Monte Carlo platform for research and clinical applications. Med Phys 2012;39 (11):6818–6837.
[17] Battistoni G et al.. The FLUKA code: an accurate simulation tool for particle therapy. Front Oncol 2016;6(116).
[18] Newhauser W et al.. Monte Carlo simulations for configuring and testing an analytical proton dose-calculation algorithm. Phys Med Biol 2007;52(15):4569.

Please cite this article as: A. Asadi, A. Akhavanallaf, S.A. Hosseini et al., Development and validation of an optimal GATE model for proton pencil-beam scanning delivery, Z Med Phys, https://doi.org/10.1016/j.zemedi.2022.10.008

[19] Paganetti H. Monte Carlo method to study the proton fluence for treatment planning. Med Phys 1998;25(12):2370–2375.
[20] Paganetti H. Monte Carlo calculations for absolute dosimetry to determine machine outputs for proton therapy fields. Phys Med Biol 2006;51(11):2801.
[21] Paganetti H et al.. Accurate Monte Carlo simulations for nozzle design, commissioning and quality assurance for a proton radiation therapy facility. Med Phys 2004;31(7):2107–2118.
[22] Parodi K et al.. Monte Carlo simulations to support start-up and treatment planning of scanned proton and carbon ion therapy at a synchrotron-based facility. Phys Med Biol 2012;57(12):3759.
[23] Robert C et al.. Distributions of secondary particles in proton and carbon-ion therapy: a comparison between GATE/Geant4 and FLUKA Monte Carlo codes. Phys Med Biol 2013;58(9): 2879–2899.
[24] Parodi K et al.. Clinical CT-based calculations of dose and positron emitter distributions in proton therapy using the FLUKA Monte Carlo code. Phys Med Biol 2007;52(12):3369–3387.
[25] Fiorini F, Schreuder N, Van den Heuvel F. Defining cyclotron-based clinical scanning proton machines in a FLUKA Monte Carlo system. Med Phys 2018;45(2):963–970.
[26] Fracchiolla F et al.. Characterization and validation of a Monte Carlo code for independent dose calculation in proton therapy treatments with pencil beam scanning. Phys Med Biol 2015;60(21):8601.
[27] Prusator M, Ahmad S, Chen Y. TOPAS Simulation of the Mevion S250 compact proton therapy unit. J Appl Clin Med Phys 2017;18 (3):88–95.
[28] Hamad MK. Bragg-curve simulation of carbon-ion beams for particle-therapy applications: A study with the GEANT4 toolkit. Nucl Eng Technol 2021;53(8):2767–2773.
[29] Padilla-Cabal F et al.. Benchmarking a GATE/Geant4 Monte Carlo model for proton beams in magnetic fields. Med Phys 2020;47 (1):223–233.
[30] Almhagen E et al.. A beam model for focused proton pencil beams. Phys Med 2018;52:27–32.
[31] Grevillot L et al.. A Monte Carlo pencil beam scanning model for proton treatment plan simulation using GATE/GEANT4. Phys Med Biol 2011;56(16):5203.
[32] Fuchs H et al.. Computer-assisted beam modeling for particle therapy. Med Phys 2021;48(2):841–851.
[33] Sánchez-Parcerisa D et al.. MultiRBE: Treatment planning for protons with selective radiobiological effectiveness. Med Phys 2019;46(9):4276–4284.
[34] Wieser HP et al.. Development of the open-source dose calculation and optimization toolkit matRad. Med Phys 2017;44(6):2556–2568.
[35] Cisternas E et al.. matRad-a multi-modality open source 3D treatment planning toolkit. World Congress on Medical Physics and Biomedical Engineering, June 7–12, 2015, Toronto, Canada. Springer; 2015.
[36] Burigo L, Jäkel O, Bangert M. matRad-An open-source treatment planning toolkit for educational purposes. Med Phys 2018;6(1).
[37] Shu H et al.. Scanned Proton Beam Performance and Calibration of the Shanghai Advanced Proton Therapy Facility. MethodsX 2019;6:1933–1943.
[38] Sheng Y et al.. Development of a Monte Carlo beam model for raster scanning proton beams and dosimetric comparison. Int J Radiat Biol 2020;96(11):1435–1442.
[39] Winterhalter C et al.. Evaluation of GATE-RTion (GATE/Geant4) Monte Carlo simulation settings for proton pencil beam scanning quality assurance. Med Phys 2020;47(11):5817–5828.
[40] Kurosu K et al.. Optimization of GATE and PHITS Monte Carlo code parameters for uniform scanning proton beam based on simulation with FLUKA general-purpose code. Nucl Instrum Methods Phys Res, Sect B 2014;336:45–54.
[41] Elia A. Characterization of the GATE Monte Carlo platform for non-isocentric treatments and patient specific treatment plan verification at MedAustron-Vienna-Austria. Université de Lyon; 2019.
[42] Elia A et al.. A GATE/Geant4 beam model for the MedAustron non-isocentric proton treatment plans quality assurance. Phys Med 2020;71:115–123.
[43] Grevillot L et al.. Optimization of GEANT4 settings for proton pencil beam scanning simulations using GATE. Nucl Instrum Methods Phys Res, Sect B 2010;268(20):3295–3305.
[44] Zahra N et al.. Influence of Geant4 parameters on dose distribution and computation time for carbon ion therapy simulation. Phys Med 2010;26(4):202–208.
[45] Andreo P. On the clinical spatial resolution achievable with protons and heavier charged particle radiotherapy beams. Phys Med Biol 2009;54(11):N205.
[46] Brice DK. Book Review: Stopping powers for electrons and positrons (ICRU report 37; International commission on radiation units and measurements, Bethesda, Maryland, USA, 1984). pp. viii+ 267, $24.00; ISBN 0-913394-31-9. Nucl Instrum Meth Phys Res B 1985;12(1):187–188.
[47] Siebert B, Schuhmacher H. Quality factors, ambient and personal dose equivalent for neutrons, based on the new ICRU stopping power data for protons and alpha particles. Radiat Prot Dosim 1995;58 (3):177–183.
[48] Schardt D et al.. Precision Bragg-curve measurements for light-ion beams in water. GSI Scientific Report 2007;373.
[49] Grevillot L et al.. GATE as a GEANT4-based Monte Carlo platform for the evaluation of proton pencil beam scanning treatment plans. Phys Med Biol 2012;57(13):4223.
[50] Grevillot L et al.. Clinical implementation and commissioning of the MedAustron Particle Therapy Accelerator for non-isocentric scanned proton beam treatments. Med Phys 2020;47(2):380–392.
[51] Schneider W, Bortfeld T, Schlegel W. Correlation between CT numbers and tissue parameters needed for Monte Carlo simulations of clinical dose distributions. Phys Med Biol 2000;45(2):459.
[52] Bourhaleb F et al.. A treatment planning code for inverse planning and 3D optimization in hadrontherapy. Comput Biol Med 2008;38 (9):990–999.
[53] Mynampati DK et al.. Application of AAPM TG 119 to volumetric arc therapy (VMAT). J Appl Clin Med Phys 2012;13(5):108–116.
[54] Mendenhall NP et al.. Early outcomes from three prospective trials of image-guided proton therapy for prostate cancer. Int J Radiat Oncol Biol Phys 2012;82(1):213–221.
[55] Zheng Y et al.. Monte Carlo study of neutron dose equivalent during passive scattering proton therapy. Phys Med Biol 2007;52(15):4481.
[56] Saini J et al.. Clinical commissioning of a pencil beam scanning treatment planning system for proton therapy. Int J Particle Therapy 2016;3(1):51–60.

Please cite this article as: A. Asadi, A. Akhavanallaf, S.A. Hosseini et al., Development and validation of an optimal GATE model for proton pencil-beam scanning delivery, Z Med Phys, https://doi.org/10.1016/j.zemedi.2022.10.008